Stabilization of a steady state in network oscillators by using diffusive connections with two long time delays

Keiji Konishi,* Hideki Kokame, and Naoyuki Hara
Department of Electrical and Information Systems, Osaka Prefecture University, 1-1 Gakuen-cho, Naka-ku, Sakai, Osaka 599-8531, Japan
(Received 26 September 2009; published 6 January 2010)

The present study shows that diffusive connections with two long-time delays can induce the stabilization of a steady state in network oscillators. A linear stability analysis shows that, if the two delay times retain a proportional relation with a certain bias, the stabilization can be achieved independent of the delay times. Furthermore, a simple systematic procedure for designing the coupling strength and the delay times in the connections is proposed. The procedure has the following two advantages: one can employ time delays as long as one wants and the stabilization can be achieved independently of its network topology. Our analytical results are applied to the well-known double-scroll circuit model on a small-world network.

DOI: 10.1103/PhysRevE.81.016201 PACS number(s): 05.45.Xt, 05.45.Gg, 05.45.Ra

I. INTRODUCTION

Coupled oscillators have attracted growing interest not only from the viewpoint of academia [1–3] but also in terms of potential engineering applications such as central pattern generators for robotic legged locomotion [4], modular robots [5], and sensor networks [6]. Amplitude death, which is a diffusive-coupling-induced stabilization of unstable fixed points in coupled oscillators, has been studied for almost 2 decades [7,8]; it is known that this phenomenon never occurs in coupled identical oscillators [8,9]. On the contrary, if the coupling signals are delayed upon connection, death can occur in coupled identical oscillators [10]. This time-delay-induced death has gained increasing attention in the field of nonlinear physics [11]. It has been observed in practical systems such as in electronic circuits [12] and thermo-optical oscillators [13]. The death has been investigated from various viewpoints [9,14–27].

Amplitude death can be regarded as a stabilization of unstable behavior; thus, it would have a great deal of potential in industry, such as in the stabilization of coupled unstable laser systems [28,29]. Naturally, we must consider that there are some practical situations in which *long* delay times in connections are inevitable; for example, if two or more unstable laser systems that are located a large distance apart are connected by optical coupling, the signal transmission between the systems inevitably includes long-time delays due to the finite propagation speed. However, it was shown that the long delay time cannot induce amplitude death [29].

Controlling chaos has been an important subject in nonlinear science. Various control methods have been proposed and applied to real systems, including electronic circuits, mechanical systems, and chemical reactions [30–34]. Among these methods, delayed feedback control (DFC), proposed by Pyragas [35], has received considerable attention not only in the field of nonlinear science [36] but also in terms of control theory [37]. The DFC method is able to stabilize two limit sets: unstable periodic orbits (UPOs) and unstable fixed points (UFPs). Stability analysis of UPOs in DFC systems is important when designing control systems, but it is not easy, because it requires solving time-periodic linear systems with time delays. In recent years, the stability of DFC systems has been intensively analyzed [38–44]. Furthermore, the stabilization of UFPs has been analytically investigated [45–49] and has been used in the fields of control theory [50] and laser systems [51]. However, the DFC method has a disadvantage in that it never stabilizes UFPs that have an odd-number property [48,49,52,73]. To overcome this disadvantage, an observer-based controller [53] and a dynamic controller [54], both of which can be designed by a systematic procedure, have been proposed.

The DFC method has been widely applied to many experimental systems, including electronic circuits and mechanical systems [36]. In such experimental situations, a delayed feedback signal is often implemented by a bucket-brigade delay-line device (i.e., a series of sample and hold circuits) or a digital computer with an AD/DA converter [55,56]. Thus, the operational speeds of these electronic devices often prevent the realization of short delay times, particularly in fast dynamical systems. Hence, for such experimental situations, there exists a need to have a feedback controller, the delay times of which can be arbitrarily long. However, as is well known, long delay times in control systems cause destabilization. Two results have been reported that provide useful information in this regard. Yanchuk *et al.* demonstrated that if a system without control is sufficiently close to a Hopf bifurcation point (i.e., weak instability), the controller can stabilize a fixed point by using long delay feedback [57]. Ahlborn and Parlitz proposed a multiple-delay feedback control (MDFC) method that has two or more delay times in the feedback signal [58–60]. The advantage of this control is that the stabilization can be achieved even if the delay times are long. MDFC has been studied on the basis of theoretical [59,61] and physical [60] viewpoints. Furthermore, it has been reported that the multiple-delay times tend to induce the stabilization in various dynamical systems, such as coupled chaotic maps [62], a neural network [63], and laser systems [64].

In previous studies, we attempted to apply the concept of MDFC to amplitude death in a pair of oscillators, but simple

*http://www.eis.osakafu-u.ac.jp/~ecs

systematic procedure for designing connection parameters could not be derived [65,66]. The main purpose of the present paper is to extend our previous research to large-scale coupled oscillators on various network topologies. Furthermore, we provide a simple systematic procedure for designing the coupling strength and the delay times in the connection. The designed connection has the following two advantages: one can employ time delays as long as one wants and the stabilization can be achieved independently of its network topology. That is, the designed connection is valid for any long delays and any network topology. Our theoretical results are applied to the well-known double-scroll circuit model on a small-world network.

II. COUPLED OSCILLATORS AND STABILITY ANALYSIS

Consider a network consisting of two-dimensional oscillators

$$\dot{Z}_j(t) = \{\mu + i\omega - |Z_j(t)|^2\}Z_j(t) + \varepsilon u_j(t), \tag{1}$$

where the complex number $Z_j(t) \in \boldsymbol{C}$ is the state variable of the jth oscillator. Here, $\mu > 0$ and $\omega > 0$ represent the degree of instability of the fixed point and the oscillator frequency, respectively. Moreover $\varepsilon \in \boldsymbol{R}$ is the coupling strength and i is denoted as $i = \sqrt{-1}$. The coupling signal $u_j(t) \in \boldsymbol{C}$ is given by

$$u_j(t) = \frac{1}{d_j}\left[\sum_{k=1}^{N} c_{jk}\{Z_k(t-\tau_1) + Z_k(t-\tau_2)\}\right] - 2Z_j(t). \tag{2}$$

Here, $\tau_{1,2} \geq 0$ are the time delays of the coupling signals and $N \geq 2$ denotes the total number of oscillators. The network topology is governed by c_{jk} as follows: if oscillator j is connected to oscillator k, then $c_{jk} = c_{kj} = 1$, otherwise $c_{jk} = c_{kj} = 0$. The self-delayed signals $Z_j(t-\tau_{1,2})$ are not allowed to be injected, that is, $c_{jj} = 0$. The number of oscillators that are connected to oscillator j, denoted as the degree of oscillator j, is written as $d_j = \Sigma_{k=1}^{N} c_{jk}$. Since coupling (2) belongs to a diffusive-type connection, the stability analysis for network oscillators can be simplified.

Oscillators (1) with coupling (2) have the homogeneous steady state: $\boldsymbol{Z}^* := [0 \ 0 \ \cdots \ 0]^T \in \boldsymbol{C}^N$. The coupled oscillators are linearized around $\boldsymbol{Z}^*$,

$$\dot{z}_j(t) = (\mu + i\omega)z_j(t) + \varepsilon\left[\frac{1}{d_j}\sum_{k=1}^{N} c_{jk}\{z_k(t-\tau_1) + z_k(t-\tau_2)\}\right] - 2\varepsilon z_j(t), \tag{3}$$

where $z_j(t) \in \boldsymbol{C}$ is the variation of oscillator j around the fixed point $Z_j^* = 0$. Substituting $z_j(t) = b_j e^{\lambda t}$ into the linearized system (3), we have

$$\lambda \boldsymbol{b} e^{\lambda t} = [\{\mu + i\omega + \varepsilon(D-2)\}\boldsymbol{I}_N - \varepsilon D\boldsymbol{L}]\boldsymbol{b}e^{\lambda t},$$

where $D := \exp(-\lambda\tau_1) + \exp(-\lambda\tau_2)$ and $\boldsymbol{b} := [b_1 \ b_2 \ \cdots \ b_N]^T$. The elements of $\boldsymbol{L}$ are given by $\{\boldsymbol{L}\}_{jk} = -c_{jk}/d_j$ for $(j \neq k)$ and $\{\boldsymbol{L}\}_{jj} = 1$. Hence, the characteristic equation of system (3) is

$$\det[\{\lambda - \mu - i\omega - \varepsilon(D-2)\}\boldsymbol{I}_N + \varepsilon D\boldsymbol{L}] = 0. \tag{4}$$

Since $\boldsymbol{L}$ is self-adjoint and positive semidefinite [22,23], it can be diagonalized as $\boldsymbol{T}^{-1}\boldsymbol{L}\boldsymbol{T} = \mathrm{diag}(\rho_1, \rho_2, \ldots, \rho_N)$, where $\boldsymbol{T}$ is a diagonal transformation matrix and ρ_q $(q = 1, 2, \ldots, N)$ are the eigenvalues of $\boldsymbol{L}$. The eigenvalues of $\boldsymbol{L}$ are given by $0 = \rho_1 < \rho_2 < \cdots < \rho_N \leq 2$ [22,23]. Thus, the characteristic Eq. (4) can be expressed as a product of characteristic equations of scalar systems

$$g(\lambda) := \prod_{q=1}^{N} \bar{g}(\lambda, \rho_q) = 0, \tag{5}$$

$$\bar{g}(\lambda, \rho_q) := \lambda - \mu + 2\varepsilon - i\omega - \varepsilon D(1 - \rho_q). \tag{6}$$

The homogeneous steady state $\boldsymbol{Z}^*$ of the coupled oscillators on network topology $\boldsymbol{c} = [c_{jk}]$ is stable if and only if all of the roots λ of Eq. (5) lie in the open left half complex plane for every $\rho_q (q = 1, 2, \ldots, N)$.

Let us investigate the roots of $\bar{g}(\lambda, \rho_q) = 0$. The stability changes only when at least one root crosses the imaginary axis. To simplify the stability analysis, we shall check the roots on the axis and estimate the stability region in a parameter space (τ_1, τ_2). By inserting $\lambda = i\lambda_I$ into $\bar{g}(\lambda, \rho_q) = 0$, we obtain its real and imaginary parts

$$\mathrm{Re}[\bar{g}(i\lambda_I, \rho_q)] = 2\varepsilon - \mu - \varepsilon(1 - \rho_q)(\cos\lambda_I\tau_1 + \cos\lambda_I\tau_2) = 0,$$

$$\mathrm{Im}[\bar{g}(i\lambda_I, \rho_q)] = \lambda_I - \omega + \varepsilon(1 - \rho_q)(\sin\lambda_I\tau_1 + \sin\lambda_I\tau_2) = 0. \tag{7}$$

The marginal stability curves are expressed using roots $\tau_{1,2}$ of the above equations. Furthermore, to investigate which direction the roots cross the imaginary axis, the sign of the real part of $d\lambda/d\tau_2$ at $\lambda = i\lambda_I$ must be checked

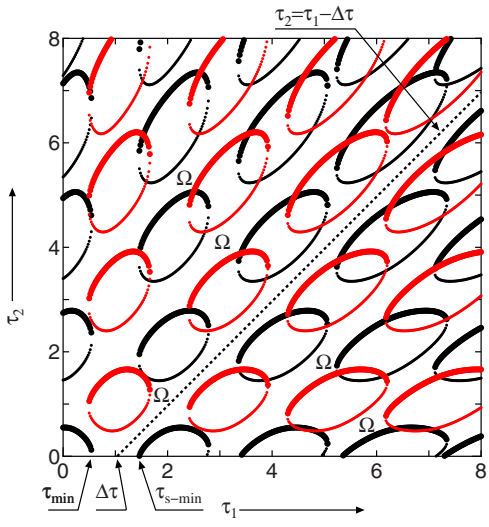

FIG. 1. (Color online) Marginal stability curves for Z^* of the pair of oscillators ($N=2$, $\rho_1=0$, $\rho_2=2$, $\mu=0.1854$, $\omega=3.0470$, $\varepsilon=\mu$). Black and red (gray) lines represent the curves for $\rho_1=0$ and $\rho_2=2$, respectively. Bold (thin) lines indicate the curves with negative (positive) terms (8).

$$\mathrm{Re}\left[\frac{d\lambda}{d\tau_2}\right]_{\lambda=i\lambda_I} = \mathrm{Re}\left[-\frac{i\lambda_I\varepsilon(1-\rho_q)\exp(-i\lambda_I\tau_2)}{1+\varepsilon(1-\rho_q)[\tau_1\exp(-i\lambda_I\tau_1)+\tau_2\exp(-i\lambda_I\tau_2)]}\right], \tag{8}$$

where $\tau_{1,2}$ and λ_I are the values satisfying Eq. (7). With increasing τ_2, a positive (negative) value of Eq. (8) corresponds to a root crossing the axis from left to right (right to left).

The above procedure is now illustrated with the simplest numerical example (i.e., a pair of oscillators: $N=2$). As the matrices $\boldsymbol{c}=[c_{jk}]$ and $\boldsymbol{L}$ are given by

$$\boldsymbol{c}=\begin{bmatrix}0 & 1\\ 1 & 0\end{bmatrix}, \quad \boldsymbol{L}=\begin{bmatrix}1 & -1\\ -1 & 1\end{bmatrix},$$

we thus obtain $\rho_1=0$ and $\rho_2=2$. The parameters are set to $\mu=0.1854$, $\omega=3.0470$, and $\varepsilon=\mu$. Figure 1 shows the marginal stability curves, estimated using the following numerical procedure: set a value for τ_1, solve $\bar{g}(\lambda,\rho_q)=0$ for τ_2 and λ_I numerically, check the sign of Eq. (8), plot (τ_1,τ_2); change the value of τ_1, and then return to the first step. The black and red (gray) lines represent the curves for $\rho_1=0$ and $\rho_2=2$, respectively. The bold (thin) lines indicate the curves with negative (positive) terms (8). These curves separate the parameter space into several regions. We know that when τ_2 increases and crosses the bold (thin) line upward, we subtract (add) 1 from (to) the number of unstable roots. Obviously, for $\tau_1=\tau_2=0$, $\bar{g}(\lambda,0)=0$ has an unstable root and $\bar{g}(\lambda,2)=0$ has no unstable root. Hence, the outside of the unstable region including the origin $\tau_1=\tau_2=0$ is the stability region denoted by Ω. It must be emphasized that the single-delay connection (i.e., $\tau_1=\tau_2$) can stabilize $\boldsymbol{Z}^*=0$ only for a small range. A multiple-delay connection, however, can stabilize it over a wide parameter region Ω.

III. DESIGN OF CONNECTIONS

This section presents a procedure for designing connection parameters such as $\tau_{1,2}$ and ε. In order to derive the procedure, the stability analysis is divided into the following three cases: (i) $\tau_1=\tau_2=0$; (ii) $\tau_1\geq 0$ and $\tau_2=0$; (iii) $\tau_2=\tau_1-\Delta\tau$, with $\tau_1\geq\Delta\tau$.

For case (i), $\tau_1=\tau_2=0$ are substituted into $\bar{g}(\lambda,\rho_q)=0$. Its root is given by $\lambda=\mu-2\varepsilon\rho_q+i\omega$; thus, $\bar{g}(\lambda,\rho_q)=0$ has an unstable root if

$$\mu-2\varepsilon\rho_q>0 \tag{9}$$

is satisfied.

For case (ii), $\tau_2=0$ is substituted into $\bar{g}(\lambda,\rho_q)=0$. Its real and imaginary parts at $\lambda=i\lambda_I$ are written by

$$\mathrm{Re}[\bar{g}(i\lambda_I,\rho_q)]=2\varepsilon-\mu-\varepsilon(1-\rho_q)(\cos\lambda_I\tau_1+1)=0, \tag{10}$$

$$\mathrm{Im}[\bar{g}(i\lambda_I,\rho_q)]=\lambda_I-\omega+\varepsilon(1-\rho_q)\sin\lambda_I\tau_1=0. \tag{11}$$

The elimination of τ_1 from Eqs. (10) and (11) yields

$$(\omega-\lambda_I)^2=(2\varepsilon-\mu)(\mu-2\varepsilon\rho_q).$$

Thus we note that if $(2\varepsilon-\mu)(\mu-2\varepsilon\rho_q)>0$, then some of the roots cross the imaginary axis at

$$\tau_1^{(\pm)}(n):=\frac{1}{\lambda_I^{(\pm)}}\left\{\pm\mathrm{Cos}^{-1}\left(\frac{\varepsilon(1+\rho_q)-\mu}{\varepsilon(1-\rho_q)}\right)+2n\pi\right\}, \tag{12}$$

$$\lambda_I^{(\pm)}:=\omega\mp\sqrt{(2\varepsilon-\mu)(\mu-2\varepsilon\rho_q)}. \tag{13}$$

Here, $\lambda_I^{(\pm)}$ are the points where the root crosses the imaginary axis. If $(2\varepsilon-\mu)(\mu-2\varepsilon\rho_q)<0$, then solutions do not exist. Hence, the root locus with $\tau_2=0$ never crosses the imaginary axis for any $\tau_1>0$. Otherwise, we have to check the direction in which the root crosses the axis. The sign of the real part of $d\lambda/d\tau_1$ at $\lambda=i\lambda_I$ is written by

$$\mathrm{Re}\left[\frac{d\lambda}{d\tau_1}\right]_{\substack{\lambda=i\lambda_I\\ \tau_2=0}}=\mathrm{Re}\left[\frac{-i\lambda_I\varepsilon(1-\rho_q)\exp(-i\lambda_I\tau_1)}{1+\varepsilon(1-\rho_q)\tau_1\exp(-i\lambda_I\tau_1)}\right]. \tag{14}$$

In cases where $\bar{g}(\lambda,\rho_q)=0$ has an unstable root at $\tau_1=\tau_2=0$ [i.e., inequality (9) holds], if the sign (14) at the smallest positive delay time of Eq. (12), denoted by $\tau_{\min}$, and that at the second smallest positive delay time, denoted by $\tau_{s\text{-}\min}$, are negative and positive, respectively, then $\bar{g}(\lambda,\rho_q)=0$ has no unstable root for $\tau_1\in[\tau_{\min},\tau_{s\text{-}\min}]$ (see Fig. 1 and the solid curve in Fig. 2).

For case (iii), τ_1 and τ_2 are assumed to have the relation

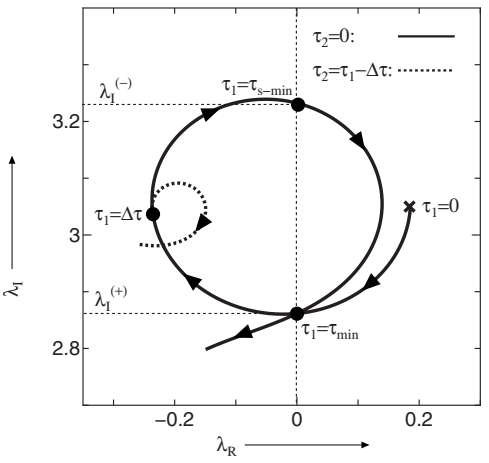

FIG. 2. Sketch of the root locus of the characteristic equation $\bar{g}(\lambda,0)=0$ with $\tau_2=0$ and small positive τ_1 near the imaginary axis ($\omega=3.0470$, $\mu=0.1854$, $\varepsilon=\mu$, $\Delta\tau=\pi/\omega$, $\tau_1\in[0,3]$).

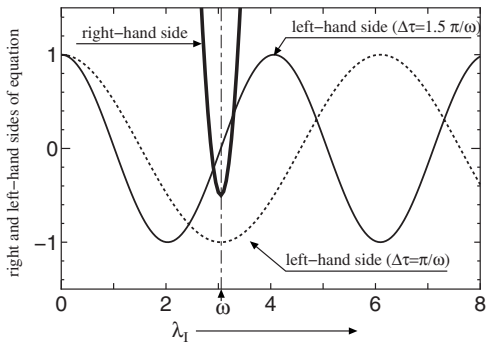

FIG. 3. Sketch of the left-hand and right-hand sides of Eq. (17) with $\rho_q=0$ ($\omega=3.0470$, $\mu=0.1854$, $\varepsilon=\mu$).

$$\tau_2 = \tau_1 - \Delta\tau, \quad \tau_1 \geq \Delta\tau, \tag{15}$$

where $\Delta\tau$ is the time difference. Substituting $\tau_2=\tau_1-\Delta\tau$ and $\lambda=i\lambda_I$ into $\bar{g}(\lambda,\rho_q)=0$ yields

$$(1+\cos\lambda_I\Delta\tau)\cos\lambda_I\tau_1 + \sin\lambda_I\Delta\tau\sin\lambda_I\tau_1 = \frac{2\varepsilon-\mu}{\varepsilon(1-\rho_q)},$$

$$(1+\cos\lambda_I\Delta\tau)\sin\lambda_I\tau_1 - \sin\lambda_I\Delta\tau\cos\lambda_I\tau_1 = \frac{\omega-\lambda_I}{\varepsilon(1-\rho_q)}. \tag{16}$$

Note that the following two statements are equivalent: the root of $\bar{g}(\lambda,\rho_q)=0$ with $\tau_2=\tau_1-\Delta\tau$ never crosses the imaginary axis and at least one equation of Eq. (16) does not hold. The second statement can be used for designing the connection. Now, both sides of Eq. (16) are squared and added and we have

$$\cos\lambda_I\Delta\tau = \frac{(2\varepsilon-\mu)^2+(\omega-\lambda_I)^2}{2\varepsilon^2(1-\rho_q)^2} - 1. \tag{17}$$

If Eq. (17) does not hold, then at least one equation of Eq. (16) does not hold. Figure 3 sketches the left-hand side and the right-hand side of Eq. (17). The parabolic bold curve is the right-hand side; the dotted (solid) cosine wave represents the left-hand side for $\Delta\tau=\pi/\omega$ ($\Delta\tau=1.5\pi/\omega$). If the parabolic curve and cosine wave do not cross, Eq. (17) does not hold. Therefore, we have only to find $\Delta\tau$ and ε such that Eq. (17) does not hold. Figure 3 illustrates that Eq. (17) does not hold for $\Delta\tau=\pi/\omega$. Thus, the root locus, the dotted curve illustrated in Fig. 2, does not cross the imaginary axis for any $\tau_1\in[\Delta\tau,\infty)$.

On the basis of the above arguments, a procedure for designing connection parameters is provided below. From the topology of network oscillators, the eigenvalues of the matrix $\boldsymbol{L}$, $\rho_q(q=1,\ldots,N)$, are estimated in advance. The steady state $\boldsymbol{Z}^*=0$ is stable independently of τ_1 if we can find the common time difference $\Delta\tau$ and strength ε for all $\rho_q(q=1,\ldots,N)$ such that the following statements are satisfied: if $\mu-2\varepsilon\rho_q>0$, all of the three inequalities, $2\varepsilon-\mu>0$, $\tau_{\min}<\Delta\tau<\tau_{s\text{-}\min}$, and $\mathrm{Re}[d\lambda/d\tau_1]_{\lambda=i\lambda_I,\tau_2=0}<0$, are satisfied; if $\mu-2\varepsilon\rho_q<0$, either $2\varepsilon-\mu>0$ or both $2\varepsilon-\mu<0$ and $\Delta\tau<\tau_{\min}$ is/are satisfied; Eq. (17) does not hold for any $\lambda_I\in\boldsymbol{R}$. The above procedure requires us to use trial-and-error testing and some numerical computations to determine $\Delta\tau$ and ε. The following section presents a simple systematic procedure that does not need such a laborious process.

IV. SIMPLE DESIGN PROCEDURE

This section describes a simple design procedure that does not require a trial- and-error testing and various numerical computations. In order to simplify our analysis, this section deals with the eigenvalues ρ_q as a parameter $\rho\in[0,2]$.

Substituting $\lambda=\lambda_R+i\lambda_I$ into $\bar{g}(\lambda,\rho)=0$, its real and imaginary parts are given by

$$\lambda_R-\mu+\varepsilon\{2-D_R(1-\rho)\}=0, \quad \lambda_I-\omega+\varepsilon D_I(1-\rho)=0, \tag{18}$$

where

$$D_R := \exp(-\lambda_R\tau_1)\cos\lambda_I\tau_1 + \exp(-\lambda_R\tau_2)\cos\lambda_I\tau_2,$$

$$D_I := \exp(-\lambda_R\tau_1)\sin\lambda_I\tau_1 + \exp(-\lambda_R\tau_2)\sin\lambda_I\tau_2.$$

For simplicity, the coupling strength ε and the delay time τ_2 are set to $\varepsilon=\mu$ and $\tau_2=0$, respectively. As a result, Eq. (18) can be reduced to

$$\lambda_R+\mu\rho-\mu(1-\rho)\exp(-\lambda_R\tau_1)\cos\lambda_I\tau_1=0,$$

$$\lambda_I-\omega+\mu(1-\rho)\exp(-\lambda_R\tau_1)\sin\lambda_I\tau_1=0. \tag{19}$$

Figure 4(a) shows the root locus of Eq. (19) for $\tau_1\geq 0$. The bold curve with circle ○ (square □) indicates the root locus with $\rho=0$ ($\rho=2$). The thin lines with ○ and □ ends are the loci for $\rho\in[0,2]$. At $\tau_1=0$, the root locus is on the segment given by $\lambda_R+i\lambda_I=\mu(1-2\rho)+i\omega$ for $\rho\in[0,2]$ [see the dotted line in Fig. 4(a)]. The segments at $\tau_1=\Delta\tau/3$, $2\Delta\tau/3$, and $\Delta\tau$ in Fig. 4(a) rotate around the point $(-\mu,\omega)$ in clockwise direction with increasing τ_1. In addition, Fig. 4(a) implies that the segment with τ_1 greater than a certain value lies in the left half plane.

Let us fix the delay times as $\tau_1=\Delta\tau=\pi/\omega$ and $\tau_2=0$. Then, the Eq. (19) has the root

$$\lambda_R+\mu\rho+\mu(1-\rho)\exp(-\lambda_R\pi/\omega)=0, \quad \lambda_I=\omega. \tag{20}$$

The segment becomes a horizontal straight line with ends that are the roots of $\lambda_R+\mu\exp(-\lambda_R\pi/\omega)=0$ and $\lambda_R+\mu[2-\exp(-\lambda_R\pi/\omega)]=0$. It should be noted that $\lambda_R=0$ does not satisfy the first equation of Eq. (20) for any $\rho\in[0,2]$. Therefore, the straight line does not intersect with the imaginary axis. The line is within the left half plane or the right half plane. It is easy to see that the root λ_R for $\rho=1$ on the line is $\lambda_R=-\mu$. Thus, these facts guarantee that the line is within the left half plane [see Fig. 4(a)]. The argument can be summarized as follows. If the coupling strength and the delay times are set to $\varepsilon=\mu$, $\tau_1=\pi/\omega$, and $\tau_2=0$, then the homogeneous steady state $\boldsymbol{Z}^*$ of the network oscillator is stable for any network topology.

The delay times are now set to $\tau_1\geq\pi/\omega$ and $\tau_2=\tau_1-\pi/\omega$. As shown in Fig. 4(b), the straight line obtained above also rotates around the point $(-\mu,\omega)$ in the clockwise

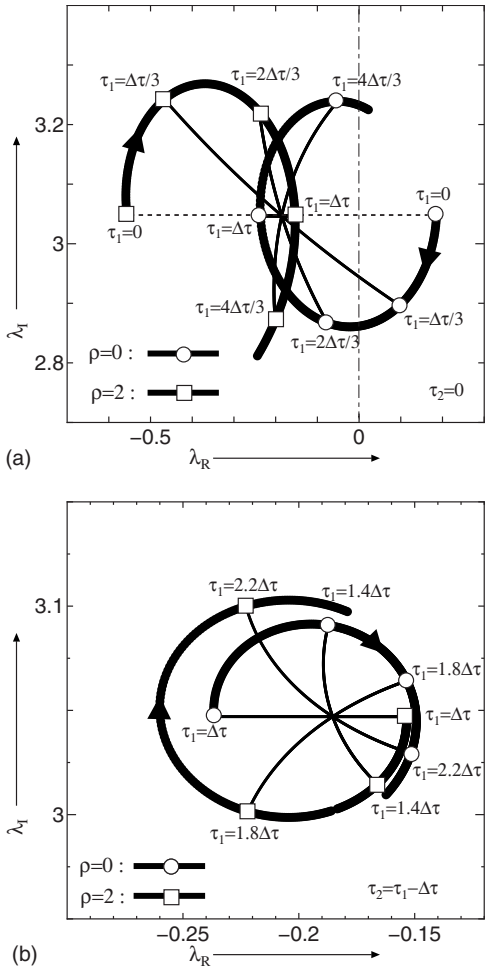

FIG. 4. Root locus of Eq. (19) (ω=3.0470, μ=0.1854, $\Delta\tau=\pi/\omega$). (a) $\tau_1 \geq 0$, $\tau_2=0$. (b) $\tau_1 \geq \Delta t$, $\tau_2=\tau_1-\Delta\tau$.

direction with increasing τ_1 and τ_2. We notice that if $\lambda_R=0$ is not a solution of Eq. (18) for any $\tau_1 \geq \pi/\omega$ and any $\rho \in [0,2]$, then the segment never intersects with the imaginary axis. This implies that the stability of $\boldsymbol{Z}^*$ remains for any $\tau_1 \geq \pi/\omega$ independently of the network topology. We shall prove below that $\lambda_R=0$ is not a solution of Eq. (18). Substituting $\Delta\tau=\pi/\omega$ and $\varepsilon=\mu$ into Eq. (17) yields

$$\cos \lambda_I \frac{\pi}{\omega} = \frac{\mu^2 + (\omega - \lambda_I)^2}{2\mu^2(1-\rho)^2} - 1. \tag{21}$$

It is clear that, if there exist no λ_I satisfying Eq. (21), then at least one equation of Eq. (18) does not hold. This shows that $\lambda_R=0$ is not a solution of Eq. (18). Now let us prove that the functions of the left-hand side and the right-hand side of Eq. (21) for λ_I do not intersect. At $\lambda_I=\omega$, these sides are -1 and $1/\{2(1-\rho)^2\}-1$, respectively. The derivative coefficients of these sides are $-\{\pi \sin(\lambda_I \pi/\omega)\}/\omega$ and $(\lambda_I-\omega)/\{\mu^2(1-\rho)^2\}$, respectively; thus, for $\omega/\mu > \pi$, the coefficient of the left-hand side is less (greater) than that of the right-hand side for any $\lambda_I > \omega$ ($\lambda_I < \omega$). This fact guarantees that Eq. (21) does not hold for any $\lambda_I \in \boldsymbol{R}$ and any $\rho \in [0,2]$.

The above arguments are summarized as follows. For $\omega/\mu > \pi$, if the coupling strength and the delay time are set to $\varepsilon=\mu$ and $\tau_2=\tau_1-\pi/\omega$, then the homogeneous steady state $\boldsymbol{Z}^*$ of the network oscillator is stable independently of the network topology for any long $\tau_1 \in [\pi/\omega, \infty)$.

V. NUMERICAL SIMULATIONS

In this section, the stability analysis mentioned in the previous sections is confirmed using a well-known chaotic-circuit model. Let us consider a network, the nodes of which are governed by the well-known double-scroll oscillator [67]

$$\dot{\boldsymbol{x}}_j(t) = \begin{bmatrix} \alpha\{x_j^{(2)}(t) - x_j^{(1)}(t) - f(x_j^{(1)}(t))\} \\ x_j^{(1)}(t) - x_j^{(2)}(t) + x_j^{(3)}(t) \\ -\beta x_j^{(2)}(t) \end{bmatrix} + \boldsymbol{u}_j(t). \tag{22}$$

The nonlinear function is described by $f(x) := bx + (b-a)\{|x-1| - |x+1|\}/2$. The circuit parameters are given by (α, β, a, b). The variable $\boldsymbol{x}_j(t) := [x_j^{(1)}(t)\ x_j^{(2)}(t)\ x_j^{(3)}(t)]^T$ is the three-dimensional system state of oscillator j at time t. The oscillator without coupling has the three fixed points, $\boldsymbol{x}_{\pm}^* := [\pm p\ \ 0\ \ \mp p]^T$ and $\boldsymbol{x}_0^* := [0\ \ 0\ \ 0]^T$, where $p := (b-a)/(b+1)$. To simplify our discussion, we focus on the stabilization of $\boldsymbol{x}_+^*$; our discussion can be similarly used for the other fixed point $\boldsymbol{x}_-^*$.

The coupling signal $\boldsymbol{u}_j(t)$ of oscillator j is described by

$$\boldsymbol{u}_j(t) = \boldsymbol{K}\left\{ \frac{1}{d_j} \left\{ \sum_{k=1}^{N} c_{jk}[\boldsymbol{x}_k(t-\tau_1) + \boldsymbol{x}_k(t-\tau_2)] \right\} - 2\boldsymbol{x}_j(t) \right\}. \tag{23}$$

Here, $\boldsymbol{K} \in \boldsymbol{R}^{3\times 3}$ is the coupling matrix that we need to design. The oscillator with connection (23) around $\boldsymbol{x}_+^*$ is governed by

$$\dot{\boldsymbol{y}}_j(t) = \boldsymbol{A}\boldsymbol{y}_j(t) + \boldsymbol{K}\left\{ \frac{1}{d_j} \left\{ \sum_{k=1}^{N} c_{jk}[\boldsymbol{y}_k(t-\tau_1) + \boldsymbol{y}_k(t-\tau_2)] \right\} - 2\boldsymbol{y}_j(t) \right\},$$

where $\boldsymbol{y}_j(t) := \boldsymbol{x}_j(t) - \boldsymbol{x}_+^*$ and $\boldsymbol{A}$ is the Jacobi matrix of the nonlinear function in Eq. (22) at $\boldsymbol{x}_+^*$.

Assume that the eigenvalues of $\boldsymbol{A}$ are given by a real eigenvalue σ and a pair of complex-conjugate eigenvalues $\mu \pm i\omega$. The transformation of a variable and suitable coupling matrix, $\boldsymbol{y}_j(t) = \boldsymbol{T}\hat{\boldsymbol{y}}_j(t)$ and $\boldsymbol{K} = \boldsymbol{T}\,\mathrm{diag}(\varepsilon, \varepsilon, 0)\boldsymbol{T}^{-1}$, allows us to obtain two independent subsystems:

$$\begin{bmatrix} \dot{\hat{y}}_j^{(1)}(t) \\ \dot{\hat{y}}_j^{(2)}(t) \end{bmatrix} = \begin{bmatrix} \mu & -\omega \\ \omega & \mu \end{bmatrix} \begin{bmatrix} \hat{y}_j^{(1)}(t) \\ \hat{y}_j^{(2)}(t) \end{bmatrix} + \varepsilon \left[\frac{1}{d_j} \sum_{k=1}^{N} c_{jk} \left\{ \begin{bmatrix} \hat{y}_k^{(1)}(t-\tau_1) \\ \hat{y}_k^{(2)}(t-\tau_1) \end{bmatrix} + \begin{bmatrix} \hat{y}_k^{(1)}(t-\tau_2) \\ \hat{y}_k^{(2)}(t-\tau_2) \end{bmatrix} \right\} \right] - 2\varepsilon \begin{bmatrix} \hat{y}_j^{(1)}(t) \\ \hat{y}_j^{(2)}(t) \end{bmatrix}, \tag{24}$$

$$\dot{\hat{y}}_j^{(3)}(t) = \sigma \hat{y}_j^{(3)}(t). \tag{25}$$

The real matrix $\boldsymbol{T}$ consists of the eigenvectors of $\boldsymbol{A}$. Obviously, system (25) behaves independently of system (24); we note that system (25) with $\sigma<0$ is a stable scalar system and that system (24) is the same as system (3). According to the simple design procedure in the preceding section, when $\omega/\mu>\pi$ and $\sigma<0$ are satisfied, we note that coupling (23) with $\boldsymbol{K}=\boldsymbol{T}\,\mathrm{diag}(\mu,\mu,0)\boldsymbol{T}^{-1}$ and $\tau_2=\tau_1-\pi/\omega$ stabilizes the fixed point $\boldsymbol{x}_+^*$ for any long $\tau_1\in[\pi/\omega,\infty)$.

Now the parameters are fixed at $(\alpha,\beta,a,b)=(9,14+2/7,-8/7,-5/7)$ in accordance with Ref. [67]. For fixed points $\boldsymbol{x}_\pm^*$, the eigenvalues of $\boldsymbol{A}$ are $\sigma\approx-3.9421$, $\mu\pm i\omega\approx0.1854\pm i3.0470$; hence, we see that $\omega/\mu>\pi$ is satisfied. The coupling matrix $\boldsymbol{K}$ designed above is given by

$$\boldsymbol{K}\approx\begin{bmatrix}+0.0031 & +0.2498 & -0.0634\\ +0.0278 & +0.1473 & +0.0097\\ +0.1006 & -0.1379 & +0.2203\end{bmatrix}.$$

In the case of $\tau_1>0$ and $\tau_2=0$, the root locus of system (24) with the designed matrix $\boldsymbol{K}$ is shown in Fig. 4(a). It can be seen that the root segment at $\tau_1=\pi/\omega$ lies in the left half plane. Further, for $\tau_1\geq\pi/\omega$ and $\tau_2=\tau_1-\pi/\omega$, the segment rotates in the clockwise direction with increasing τ_1 and τ_2, but never cross the imaginary axis, as shown in Fig. 4(b). These numerical results agree well with the stability analysis.

As a numerical example, we employ a small-world network [68]. Every node is coupled to its nearest neighbors (i.e., one-dimensional ring-type lattice with periodic boundary) and N_c shortcuts, the ends of which are randomly chosen pairs of nodes, are added to the lattice. In particular, the elements c_{jk} are given by the following procedure: $c_{j(j+1)}=c_{(j+1)j}=1$, $\forall\ j\in[1,N-1]$, and $c_{1N}=c_{N1}=1$ for the implementation of a one-dimensional ring-type lattice; choose N_c pairs of nodes $\{j,k\}$ randomly and connect them as $c_{jk}=c_{kj}=1$; set the other elements to zero. It is easy to check that matrix $\boldsymbol{L}$ used in Eq. (4) is self-adjoint and positive semifinite. Thus, the matrix $\boldsymbol{K}$ and the delay difference $\Delta\tau$ based on our stability analysis can be applied to the coupled double-scroll oscillators on the small-world network. Figure 5(a) shows the time-series data of the oscillators coupled by a single long time-delay connection ($\tau_1=\tau_2=20$). The initial condition $\boldsymbol{x}_j(t-\tau)=\boldsymbol{x}_0$, $\forall\ \tau\in[0,\tau_1]$ is randomly chosen within $|x_0^{(1,2,3)}|<0.1$. The state variables of the first oscillator, $x_1^{(1)}$, $x_1^{(2)}$, and $x_1^{(3)}$, do not converge on a fixed point. In contrast, from Fig. 5(b), it can be seen that the connection with two time delays, $\tau_1=20$ and $\tau_2=20-\pi/\omega$, induces the stabilization of $\boldsymbol{x}_+^*$. According to our stability analysis, the stabilization remains even if the delay times are extended as long as one wants.

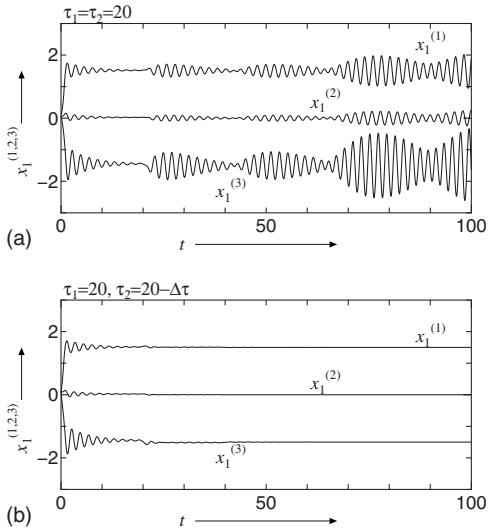

FIG. 5. Time-series data of the first oscillator: $x_1^{(1,2,3)}$ ($N=50$, $N_c=5$). (a) Single time delay ($\tau_1=\tau_2=20$). (b) Two time delays ($\tau_1=20$, $\tau_2=20-\pi/\omega$).

VI. DISCUSSIONS

This section discusses the relation between our results and those of related studies. To our knowledge, very little work is currently available in the published literature on phenomena regarding oscillators coupled with multiple-delay connections. However, if our results are restricted to the stabilization of isolated oscillators, they would be related to several previous studies on multiple-delay systems.

Let us restrict our results to the stabilization of isolated oscillator: $N=1$, $c_{11}=1$, $d_1=1$, and $\rho_1=0$. The characteristic Eq. (5) is simplified as $g(\lambda):=\bar{g}(\lambda,0)=0$. Thus, it is clear that our results are also valid for the isolated oscillator, since the simplified characteristic equation describes a specific case of Eq. (5) with $N=1$ and $\rho_1=0$. For $\mu=0.1854$ and $\omega=3.0470$, the marginal stability curves for the isolated oscillator are shown as black curves in Fig. 1. Evidently, the simple design procedure is still valid. For $\omega/\mu>\pi$, if $\varepsilon=\mu$, $\tau_1\geq\pi/\omega$, and $\tau_2=\tau_1-\pi/\omega$, then the fixed point $Z^*=0$ of the oscillator is stable for any $\tau_1\in[\pi/\omega,\infty)$.

Hastings analyzed the stability of a fixed point in a modified Lotka-Volterra model including two time delays ($\tau_{1,2}$) [69,70]. Although the characteristic equation of this model has the two time delays, the structure of this equation is quite different from that of $\bar{g}(\lambda,\rho_q)=0$ in Eq. (6). The stability region in the parameter space (τ_1 vs τ_2) was numerically provided; we can see a long band of stability in this space. Hence, there would exist the relation such as Eq. (15) in this band. However, no analytical investigation on this band is available.

Blyuss *et al.* showed that unstable steady states in neutral time-delayed systems with τ_1 can be stabilized by the delayed feedback control with τ_2 [71]. There is a difference between the characteristic equation of this feedback system and $\bar{g}(\lambda,0)=0$ in Eq. (6). In the former, the coefficient of $\exp(-\lambda\tau_1)$ depends on λ; in contrast, both coefficients of $\exp(-\lambda\tau_1)$ and $\exp(-\lambda\tau_2)$ in the latter case are independent of λ. Although this difference is significant in terms of stability analysis, the stability region in the parameter space (τ_1 vs τ_2) in Ref. [71] is quite similar to the region with black curves ($\rho_q=0$) shown in Fig. 1.

Ahlborn and Parlitz proposed MDFC method to stabilize unstable steady states of isolated oscillators [58,59]. As the characteristic equation of the MDFC system is equal to $\bar{g}(\lambda,0)=0$ in Eq. (6), the stability region in the parameter

space (τ_1 vs τ_2) in Refs. [58,59] is also the same as the region bounded by black curves ($\rho_q=0$) shown in Fig. 1. Although the MDFC system has a single characteristic equation $\bar{g}(\lambda,0)=0$, the characteristic Eq. (5) is a product of N functions $\bar{g}(\lambda,\rho_q)$, $(q=1,\ldots,N)$. We may regard the stabilization with the MDFC as a specific case of amplitude death in oscillators (1) coupled by connection (2).

Lu *et al.* investigated the MDFC systems with two time delays from the viewpoints of control system theory [72]. They considered general dynamical systems and provided a systematic procedure based on the linear matrix inequality technique to design the feedback gain matrix. This procedure is useful for designing the gain; however, the two delays cannot be designed using this procedure. In other words, a trial-and-error work is needed to design them. Since this procedure is derived on the basis of the Lyapunov function, the stability analysis would be conservative.

From the previous studies [58,59,69–71] mentioned above, we note that the stability regions in the parameter space (τ_1 vs τ_2) are quite similar despite of the difference in their characteristic equations. We believe that this fact is worth investigating in detail; specifically, a general time-delayed system incorporating the work of previous studies should be analyzed theoretically. Furthermore, it would be important to develop a systematic procedure for designing long delay times for the general systems.

The present paper has investigated the stability of networks on the assumption under which all of the oscillators are identical. Although this assumption simplifies our stability analysis, it would not be practical for physical systems. Thus, the parameter mismatch of oscillators should be taken into the consideration in analyzing the stability. Further studies are needed to clarify the influence of the mismatch on the stability.

VII. CONCLUSION

This paper has shown that multiple long delay connections can induce the stabilization of a steady state in network oscillators. A simple systematic procedure for designing the coupling strength and the delay-time relation was proposed. The designed connection is valid for any long delay times and any network topology. Our analytical results are applied to the well-known double-scroll circuit model on a small-world-type network.

ACKNOWLEDGMENT

K.K. thanks Dr. P. Hövel for providing useful information on delayed systems.

[1] T. Endo and S. Mori, IEEE Trans. Circuits Syst. **23**, 100 (1976).
[2] Y. Nishio and A. Ushida, IEEE Trans. Circuits Syst., I: Fundam. Theory Appl. **42**, 678 (1995).
[3] A. Pikovsky, M. Rosenblum, and J. Kurths, *Synchronization* (Cambridge University Press, London, 2001).
[4] P. Holmes, R. Full, D. Koditschek, and J. Guckenheimer, SIAM Rev. **48**, 207 (2006).
[5] A. Ishiguro, M. Shimizua, and T. Kawakatsub, Rob. Auton. Syst. **54**, 641 (2006).
[6] Y.-W. Hong and A. Scaglione, IEEE J. Sel. Areas Commun. **23**, 1085 (2005).
[7] Y. Yamaguchi and H. Shimizu, Physica D **11**, 212 (1984).
[8] D. Aronson, G. Ermentout, and N. Kopell, Physica D **41**, 403 (1990).
[9] K. Konishi, Phys. Lett. A **341**, 401 (2005).
[10] D. V. Ramana Reddy, A. Sen, and G. L. Johnston, Phys. Rev. Lett. **80**, 5109 (1998).
[11] S. Strogatz, Nature (London) **394**, 316 (1998).
[12] D. V. Ramana Reddy, A. Sen, and G. L. Johnston, Phys. Rev. Lett. **85**, 3381 (2000).
[13] R. Herrero, M. Figueras, J. Rius, F. Pi, and G. Orriols, Phys. Rev. Lett. **84**, 5312 (2000).
[14] D. V. Ramana Reddy, A. Sen, and G. L. Johnston, Physica D **129**, 15 (1999).
[15] K. Konishi, Phys. Rev. E **70**, 066201 (2004).
[16] R. Dodla, A. Sen, and G. L. Johnston, Phys. Rev. E **69**, 056217 (2004).
[17] M. Mehta and A. Sen, Phys. Lett. A **355**, 202 (2006).
[18] K. Konishi, Phys. Rev. E **68**, 067202 (2003).
[19] K. Konishi, Int. J. Bifurcation Chaos Appl. Sci. Eng. **17**, 2781 (2007).
[20] F. M. Atay, Phys. Rev. Lett. **91**, 094101 (2003).
[21] F. Atay, Physica D **183**, 1 (2003).
[22] F. M. Atay, J. Differ. Equations **221**, 190 (2006).
[23] F. M. Atay and O. Karabacak, SIAM J. Appl. Dyn. Syst. **5**, 508 (2006).
[24] A. Prasad, Phys. Rev. E **72**, 056204 (2005).
[25] K. Konishi, K. Senda, and H. Kokame, Phys. Rev. E **78**, 056216 (2008).
[26] J. Yang, Phys. Rev. E **76**, 016204 (2007).
[27] Y. Song, J. Wei, and Y. Yuan, J. Nonlinear Sci. **17**, 145 (2007).
[28] S. Tang, R. Vicente, M. C. Chiang, C. R. Mirasso, and J.-M. Liu, IEEE J. Sel. Top. Quantum Electron. **10**, 936 (2004).
[29] R. Vicente, S. Tang, J. Mulet, C. R. Mirasso, and J.-M. Liu, Phys. Rev. E **73**, 047201 (2006).
[30] G. Chen and X. Dong, *From Chaos to Order* (World Scientific, Singapore, 1998).
[31] H. Schuster, *Handbook of Chaos Control* (Wiley-VCH, New York, 1999).
[32] E. Scholl and H. Schuster, *Handbook of Chaos Control* (Wiley-VCH, New York, 2008).
[33] B. R. Andrievskii and A. L. Fradkov, Autom. Remote Control (Engl. Transl.) **64**, 673 (2003).
[34] B. R. Andrievskii and A. L. Fradkov, Autom. Remote Control (Engl. Transl.) **65**, 505 (2004).
[35] K. Pyragas, Phys. Lett. A **170**, 421 (1992).
[36] K. Pyragas, Philos. Trans. R. Soc. London, Ser. A **364**, 2309 (2006).
[37] K. Gu and S. Niculescu, ASME J. Dyn. Syst., Meas., Control

125, 158 (2003).
[38] H. Nakajima, Phys. Lett. A **232**, 207 (1997).
[39] W. Just, Physica D **142**, 153 (2000).
[40] B. Fiedler, V. Flunkert, M. Georgi, P. Hövel, and E. Schöll, Phys. Rev. Lett. **98**, 114101 (2007).
[41] W. Just, B. Fiedler, M. Georgi, V. Flunkert, P. Hövel, and E. Schöll, Phys. Rev. E **76**, 026210 (2007).
[42] C. M. Postlethwaite and M. Silber, Phys. Rev. E **76**, 056214 (2007).
[43] K. Pyragas, Phys. Rev. Lett. **86**, 2265 (2001).
[44] K. Pyragas, V. Pyragas, I. Z. Kiss, and J. L. Hudson, Phys. Rev. E **70**, 026215 (2004).
[45] A. Chang, J. C. Bienfang, G. M. Hall, J. R. Gardner, and D. J. Gauthier, Chaos **8**, 782 (1998).
[46] P. Hövel and E. Schöll, Phys. Rev. E **72**, 046203 (2005).
[47] T. Dahms, P. Hövel, and E. Schöll, Phys. Rev. E **76**, 056201 (2007).
[48] H. Kokame, K. Hirata, K. Konishi, and T. Mori, Int. J. Control **74**, 537 (2001).
[49] H. Kokame, K. Hirata, K. Konishi, and T. Mori, IEEE Trans. Autom. Contr. **46**, 1908 (2001).
[50] K. Hirata, H. Kokame, K. Konishi, and H. Fujita, Proceedings of American Control Conference, 2001, pp. 25–27.
[51] V. Z. Tronciu, H.-J. Wünsche, M. Wolfrum, and M. Radziunas, Phys. Rev. E **73**, 046205 (2006).
[52] T. Ushio, IEEE Trans. Circuits Syst., I: Fundam. Theory Appl. **43**, 815 (1996).
[53] K. Konishi and H. Kokame, Phys. Lett. A **248**, 359 (1998).
[54] S. Yamamoto, T. Hino, and T. Ushio, IEEE Trans. Circuits Syst., I: Fundam. Theory Appl. **48**, 785 (2001).
[55] A. Kittel *et al.*, Z. Naturforsch., A: Phys. Sci. **49**, 843 (1994).
[56] T. Hikihara and T. Kawagoshi, Phys. Lett. A **211**, 29 (1996).
[57] S. Yanchuk, M. Wolfrum, P. Hövel, and E. Schöll, Phys. Rev. E **74**, 026201 (2006).
[58] A. Ahlborn and U. Parlitz, Phys. Rev. Lett. **93**, 264101 (2004).
[59] A. Ahlborn and U. Parlitz, Phys. Rev. E **72**, 016206 (2005).
[60] A. Ahlborn and U. Parlitz, Opt. Lett. **31**, 465 (2006).
[61] K. Konishi and H. Kokame, Proceedings of the 15th International IEEE Workshop on Nonlinear Dynamics of Electronic Systems, 2007, pp. 249–252.
[62] C. Masoller and A. C. Martí, Phys. Rev. Lett. **94**, 134102 (2005).
[63] T. Omi and S. Shinomoto, Phys. Rev. E **77**, 046214 (2008).
[64] A. Tobbens and U. Parlitz, Phys. Rev. E **78**, 016210 (2008).
[65] K. Konishi and H. Kokame, Proceedings of the International Symposium on Nonlinear Theory and its Applications, 2008, pp. 528–531.
[66] K. Konishi, H. Kokame, and N. Hara, Proceedings of the Second IFAC Meeting Related to Analysis and Control of Chaotic Systems, 2009 (unpublished).
[67] T. Matsumoto, L. Chua, and M. Komuro, IEEE Trans. Circuits Syst. **32**, 797 (1985).
[68] C. Moore and M. E. J. Newman, Phys. Rev. E **61**, 5678 (2000).
[69] A. Hastings, J. Math. Biol. **21**, 35 (1984).
[70] W. Murdoch, R. Nisbet, S. Blythe, W. Gurney, and J. D. Reeve, Am. Nat. **129**, 263 (1987).
[71] K. Blyuss, Y. Kyrychko, P. Hövel, and E. Schöll, Eur. Phys. J. B **65**, 571 (2008).
[72] J. Lu, Z. Ma, and L. Li, Commun. Nonlinear Sci. Numer. Simul. **14**, 3037 (2009).
[73] Although a counter example of the odd-number property for UPOs on time-continuous systems has been reported in [40], the property is valid for UFPs [48,49].